PHYSICAL REVIEW B VOLUME 13, NUMBER 4 15 FEBRUARY 1976

# Theory of electroabsorption by anisotropic and layered semiconductors. I. Two-dimensional excitons in a uniform electric field*

Frank L. Lederman† and John D. Dow
*Department of Physics and Materials Research Laboratory, University of Illinois, Urbana-Champaign, Urbana, Illinois 61801*
(Received 2 September 1975)

A basis for the theory of electroabsorption by excitons in anisotropic and layered semiconductors is developed, in which the excitons are assumed to be two dimensional. The effective-mass equation for a two-dimensional exciton in a uniform electric field of arbitrary strength is solved exactly (numerically), and the electroabsorption spectra computed for direct allowed, direct "forbidden" (second class), and indirect allowed transitions. The calculated spectra are compared with corresponding spectra for three-dimensional excitons and with spectra calculated neglecting the electron-hole interaction. The results are tabulated in a form that facilitates comparison with experimental data.

## I. INTRODUCTION

Layered materials, with their ease of intercalation,[1] favorable lubrication properties, tendency toward Fermi-surface-driven instabilities,[2,3] and observable charge-density waves,[4] have captured the attention of many physicists in recent years. The layered semiconductors, particularly the transition-metal dichalcogenides, have exhibited optical and electro-optical spectra with well-defined bound exciton levels—although those levels have often frustrated attempts to interpret them as caused by either two- or three-dimensional excitons.[5–7]

In this paper, we establish a framework for treating the electric field perturbed excitons in layered semiconductors by solving exactly the Schrödinger equation for a two-dimensional hydrogenic exciton in a uniform electric field of arbitrary strength. These solutions can then be taken together with corresponding solutions for three-dimensional excitons[8–11] as starting points for the interpolation between two and three dimensions that will be necessary for the proper description of the layered materials. This interpolation, however, is a good deal less trivial than one might guess, because standard approximations are applicable only to limited ranges of field strength and photon energy.[12,13] Hence we shall confine our attention here to the case of well-separated layers, for which the two-dimensional approximation is apt.

Section II contains the elementary formalism of the theory of absorption by two-dimensional excitons; Sec. III discusses the separation of the effective-mass equation and, together with Appendix makes contact with previous three-dimensional exciton work. Various limiting cases of exciton theory are recalled in Sec. IV, and our results are presented in Sec. V. Interpolation formulas for analyzing data are given in Sec. VI and our results are summarized in Sec. VII.

## II. FORMALISM

In this section, we derive Elliott's formula for the coefficient of optical absorption by excitons in a layered material. The absorption coefficient $K_A(\omega)$ is related to the imaginary part of the dielectric function $\epsilon_2(\omega)$ by

$$K_A(\omega) = \omega\epsilon_2(\omega)/c\eta'(\omega) , \tag{2.1}$$

where $\omega$ is the photon frequency, $c$ is the speed of light, and $\eta'(\omega)$ is the (real) index of refraction. Assuming dipole transitions, we can write $\epsilon_2(\omega)$ (loosely called the optical absorption) in terms of the eigenstates $|n\rangle$ of the unperturbed Hamiltonian:

$$\epsilon_2(\omega) = \frac{4\pi^2}{\omega^2 AL} \lim_{\vec{q}\to 0} \sum_n |\langle 0|\hat{\epsilon}\cdot\vec{J}(\vec{q})|n\rangle|^2 \delta(\hbar\omega - \hbar\omega_{n0}) . \tag{2.2}$$

Here $V=AL$ is the crystal volume, $\hat{\epsilon}$ is the photon polarization, $\vec{J}(\vec{q})$ is the Fourier transform of the current operator, $|0\rangle$ is the ground state of the crystal in the presence of an electric field $\vec{F}$, but not of the photon, and $\hbar\omega_{n0}$ is the excitation energy of the excited state $|n\rangle$.

Taking $|n\rangle$ to be exciton states of total momentum $\vec{K}$ and internal quantum numbers $\nu$ [weighted by an envelope function $U_{cv\nu\vec{K}}(\vec{R})$], and expressing $|\vec{K}cv\nu\rangle$ in terms of the Wannier states centered at lattice sites $\vec{R}^0$, we have[11]

$$\langle 0|\hat{\epsilon}\cdot\vec{J}(\vec{q})|\vec{K}cv\nu\rangle = \frac{eA^{1/2}L^{1/2}}{mN^{1/2}} \sum_{\vec{R}^0_{eh}} U_{cv\nu\vec{K}}(\vec{R}^0_{eh}) \times \sum_{\vec{R}^0_h} e^{i\vec{K}\cdot\vec{R}^0_h} \langle v, \vec{R}^0_h| e^{-i\vec{q}\cdot\vec{r}}\hat{\epsilon}\cdot\vec{p}|c, \vec{R}^0_h + \vec{R}^0_{eh}\rangle . \tag{2.3}$$

Here $e$, $m$ are the charge and mass of the elec-

tron, $N$ is the number of unit cells, and $c$ and $v$ refer to the periodic parts of the conduction- and valence-band wave functions, respectively. It is useful to insert a complete set of single particle Bloch states $|n, (\vec{k}+\vec{K})_{\parallel}\rangle$, where the $\parallel$ and $\perp$ symbols refer to components parallel to and perpendicular to the layers, respectively. Then Eq. (2.3) can be written

$$\langle 0|\hat{\epsilon}\cdot\vec{J}(\vec{q})|\vec{K}cv\nu\rangle \frac{eA^{1/2}L^{1/2}}{mN}\sum_{\vec{R}^0_{eh}} U_{cv\nu\vec{K}}(\vec{R}^0_{eh}) \sum_{R^0_{h\perp}\vec{k}_{\parallel}} \langle v, \vec{k}_{\parallel}\vec{R}^0_{h\perp}|e^{-i\vec{q}\cdot\vec{r}}\hat{\epsilon}\cdot\vec{p}|c, (\vec{k}+\vec{K})_{\parallel}(\vec{R}^0_h+\vec{R}^0_{eh})_{\perp}\rangle e^{-i(\vec{k}+\vec{K})\cdot\vec{R}^0_{eh}} . \tag{2.4}$$

The maximum overlap will occur for $R^0_{eh,\perp}=0$ and $k_{\perp}$ can be expanded about the minimum point ($\vec{k}_0=0$). Then the sum over $k_{\perp}$ in Eq. (2.4) results in a $\delta$ function in $R^0_{eh,\perp}$, and we have [from Eq. (2.2)] the Elliott formula[14]

$$\epsilon_2(\omega)=\frac{4\pi^2e^2}{m^2\omega^2}\lim_{\substack{\vec{K}=0\\ \vec{k}_{0,\parallel}=0\\ R^0_{eh,\perp}=0}} \left|\langle v, \vec{k}_{0,\parallel}\vec{R}^0_{h\perp}|e^{-i\vec{q}\cdot\vec{r}}\hat{\epsilon}\cdot\vec{p}|c, (\vec{k}_0+\vec{K})_{\parallel}(\vec{R}^0_h+\vec{R}^0_{eh})_{\perp}\rangle\right|^2 \sum_{\nu}|U_{cv\nu\vec{K}}(0)|^2\delta(\hbar\omega-E_{gap}-E_{cv\nu\vec{K}})$$

$$\equiv C_{02}|U(0)|^2 S(\hbar\omega-E_{gap}) . \tag{2.5}$$

This is the principal result of Elliott's theory of direct allowed transitions to exciton states.[14] Similar expressions [Eqs. (4.12) and (5.1)] hold for direct "forbidden" and for indirect transitions. If the one-electron matrix element is assumed independent of energy (at least for energies within a few exciton binding energies of the band gap), then the absorption line shape is completely determined by the envelope wave function $U(R)$ and the density of states $S(E)$. These functions are obtained by solving the effective-mass Schrödinger equation.

## III. SEPARATION OF EFFECTIVE-MASS EQUATION

The exciton effective-mass Schrödinger equation is

$$\left(\frac{-\hbar^2}{2\mu_x}\frac{\partial^2}{\partial x^2}-\frac{\hbar^2}{2\mu_y}\frac{\partial^2}{\partial y^2}-\frac{\hbar^2}{2M_z}\frac{\partial^2}{\partial z^2}-\frac{e^2}{\epsilon r}-eFx\right)U=EU, \tag{3.1}$$

where the $x$ axis is taken in the direction of the applied electric field $F$ and is perpendicular to the normal vector of the layers, $2\pi\hbar$ is Planck's constant, $e=-|e|$, $\epsilon$ is the static dielectric constant of the semiconductor (approximated as scalar), and $\mu_x$, $\mu_y$, and $M_z$ are the eigenvalues of the effective-mass tensor. Here we consider an isotropic layered semiconductor in which the layers are well separated:

$$\mu_x=\mu_y\equiv\mu , \qquad M_z=\infty . \tag{3.2}$$

Focusing our attention on a single layer and taking the units of energy and length to be the exciton Rydberg and Bohr radius

$$R=e^2/2\epsilon a \tag{3.3}$$

and

$$a=\hbar^2\epsilon/\mu e^2 , \tag{3.4}$$

we find

$$(-\nabla^2_{x,y}-2/\rho+fx)U=EU , \tag{3.5}$$

where we have defined the reduced field $f$ by

$$\vec{F}\equiv(fR/|e|a)\hat{x} . \tag{3.6}$$

Qualitatively, a reduced field $f$ of order unity ionizes the $1s$ exciton. Transformation to parabolic cylindrical coordinates[15]

$$\xi=\rho+x, \qquad \zeta=\rho-x ,$$
$$x=\tfrac{1}{2}(\xi-\zeta), \qquad y=\sqrt{\xi\zeta} , \tag{3.7}$$

leads to the separation of the Schrödinger equation:

$$\chi_1''-V_1(\xi)\chi_1(\xi)=0 , \tag{3.8a}$$

$$\chi_2''-V_2(\zeta)\chi_2(\zeta)=0 , \tag{3.8b}$$

where we have

$$U(x,y)=\chi_1(\xi)\chi_2(\zeta)/(\xi\zeta)^{1/4} , \tag{3.9}$$

$$V_1(\xi)=-\left(\frac{1-m^2}{4\xi^2}+\frac{t}{\xi}+\frac{E}{4}-\frac{f\xi}{8}\right), \tag{3.10a}$$

and

$$V_2(\zeta)=-\left(\frac{1-m^2}{4\zeta^2}+\frac{J-t}{\zeta}+\frac{E}{4}+\frac{f\zeta}{8}\right) . \tag{3.10b}$$

Here $t$ is a separation constant (with a discrete spectrum), $J\equiv1$,[16] and we have $m=\pm\frac{1}{2}$ for two dimensions. The purpose of writing these equations in this form is to facilitate comparison with the three-dimensional case, where the separated Schrödinger equations (3.8) are identical, with the exceptions that the coordinates $\xi$ and $\zeta$ are somewhat differently defined, and the wave function is somewhat differently normalized. Thus, with some minor modifications detailed in Appendix, the problem of computing exact (numerical) solu-

tions of the effective-mass equation has been solved.

## IV. LIMITING CASES

In discussing the calculated spectra, it will be useful to compare with several limiting cases, depending on the dimensionality $d$ ($=2$ or 3), electric field strength ($f$), and electron-hole interaction strength ($J$). Analytic results are available in the following cases

### A. Allowed direct transitions

$$\epsilon_2(\omega) = C_0 |U(0)|^2 S(E) , \tag{4.1}$$

$$E \equiv \hbar\omega - E_{\text{gap}} , \tag{4.2}$$

$$\beta \equiv -Ef^{-2/3} . \tag{4.3}$$

#### 1. Two dimensions ($d=2$)

$$C_{02} = \frac{4\pi e^2}{m^2\omega^2}\frac{1}{Ra^2}|\langle v,0|\hat{\epsilon}\cdot\vec{p}|c,0\rangle|^2 . \tag{4.4}$$

*a. Zero-field zero electron-hole interaction* ($f=J=0$):

$$\epsilon_2 = (C_{02}/4\pi)\Theta(E) , \tag{4.5}$$

where $\Theta(E)$ is the unit step function.

*b. Franz-Keldysh effect: finite-field zero electron-hole interaction*[17] ($f>0$, $J=0$):

$$\epsilon_2 = \frac{C_{02}}{4\pi}\int_{2^{2/3}\beta}^{\infty}\text{Ai}(t)\,dt , \tag{4.6}$$

where the Airy function Ai($t$) is normalized as by Abramowitz and Stegun.[18]

*c. Zero-field excitons*[19,20] ($f=0$, $J=1$):

$$\epsilon_2 = \frac{C_{02}}{\pi}\sum_{n=1}^{\infty}\frac{1}{(n-\frac{1}{2})^3}\delta(E+(n-\tfrac{1}{2})^{-2}) + \frac{C_{02}\Theta(E)}{2\pi}\frac{1}{1+e^{-2\pi/\sqrt{E}}} . \tag{4.7}$$

#### 2. Three dimensions ($d=3$)

$$C_{03} = \lim_{\vec{k}_0\to 0}\frac{4\pi e^2}{m^2\omega^2}\frac{1}{Ra^3}|\langle c,\vec{k}_0|\hat{\epsilon}\cdot\vec{p}|v,\vec{k}_0\rangle|^2 . \tag{4.8}$$

*a. Zero-field zero electron-hole interaction* ($f=J=0$):

$$\epsilon_2 = (C_{03}/4\pi)\sqrt{E}\,\Theta(E) . \tag{4.9}$$

*b. Franz-Keldysh effect*[21] ($f>0$, $J=0$):

$$\epsilon_2 = (C_{03}/4\pi)f^{1/3}[|\text{Ai}'(\beta)|^2 - \beta|\text{Ai}(\beta)|^2] . \tag{4.10}$$

*c. Zero-field excitons*[14] ($f=0$, $J=1$):

$$\epsilon_2 = \frac{C_{03}}{\pi}\sum_{n=1}^{\infty}\frac{1}{n^3}\delta(E+n^{-2}) + \frac{C_{03}}{2\pi}\frac{\Theta(E)}{1-e^{-2\pi/\sqrt{E}}} . \tag{4.11}$$

### B. "Forbidden" direct transitions

$$\epsilon_2 = C_1|\nabla U(0)|^2 S(E) . \tag{4.12}$$

#### 1. Two dimensions ($d=2$)

$$C_{12} = \lim_{\substack{\vec{k}_{0,\parallel}\to 0\\ R^0_{h\perp}\to 0}}\frac{4\pi e^2}{m^2\omega^2 Ra^4}\left|\left\langle c,\vec{k}_{0,\parallel}\vec{R}^0_{h\perp}\right|\sum_i\left(\frac{\vec{p}|i\rangle\langle i|\hat{\epsilon}\cdot\vec{p}}{E_c-E_i} + \frac{\hat{\epsilon}\cdot\vec{p}|i\rangle\langle i|p}{E_v-E_i}\right)\left|v,k_{0,\parallel}\vec{R}^0_{h\perp}\right\rangle\right|^2 . \tag{4.13}$$

*a. Zero-field zero electron-hole interaction* ($f=J=0$):

$$\epsilon_2 = (C_{12}/4\pi)E\Theta(E) . \tag{4.14}$$

*b. Franz-Keldysh effect*[17] ($f>0$, $J=0$):

$$\epsilon_2\ (\text{parallel to field}) = \frac{-C_{12}}{8\pi}\left(\frac{f}{2}\right)^{2/3}\times\left(3\text{Ai}'(2^{2/3}\beta) + 2^{2/3}\beta\int_{2^{2/3}\beta}^{\infty}\text{Ai}(t)\,dt\right) , \tag{4.15}$$

$$\epsilon_2\ (\text{perpendicular to field}) = \frac{-C_{12}}{8\pi}\left(\frac{f}{2}\right)^{2/3}\times\left(2^{2/3}\beta\int_{2^{2/3}\beta}^{\infty}\text{Ai}(t)\,dt + \text{Ai}'(2^{2/3}\beta)\right) , \tag{4.16}$$

*c. Zero-field excitons* ($f=0$, $J=1$):

$$\epsilon_2 = \frac{2C_{12}}{\pi}\sum_{n=2}^{\infty}\frac{n(n-1)}{(n-\frac{1}{2})^5}\delta(E+(n-\tfrac{1}{2})^{-2}) + \frac{C_{12}\Theta(E)}{4\pi}\frac{E+4}{1+e^{-2\pi/\sqrt{E}}} . \tag{4.17}$$

#### 2. Three dimensions ($d=3$)

$$C_{13} = \lim_{\vec{k}_0\to 0}\frac{4\pi e^2\hbar^2}{m^2\omega^2 Ra^5}\left|\left\langle c,\vec{k}_0\right|\sum_i\left(\frac{\vec{p}|i\rangle\langle i|\hat{\epsilon}\cdot\vec{p}}{E_c-E_i} + \frac{\hat{\epsilon}\cdot\vec{p}|i\rangle\langle i|\vec{p}}{E_v-E_i}\right)\left|v,k_0\right\rangle\right|^2 . \tag{4.18}$$

*a. Zero-field zero electron-hole interaction* ($f=J=0$):

$$\epsilon_2 = (C_{13}/12\pi^2)E^{3/2}\Theta(E) . \tag{4.19}$$

*b. Franz-Keldysh effect*[17] ($f>0$, $J=0$):

$$\epsilon_2\ (\text{parallel to field}) = (C_{13}/12\pi)\times f[\beta^2\text{Ai}^2(\beta) - 2\text{Ai}(\beta)\text{Ai}'(\beta) - \beta|\text{Ai}'(\beta)|^2], \tag{4.20}$$

$$\epsilon_2\ (\text{perpendicular to field}) = (-C_{13}/24\pi)\times f\{2\beta[|\text{Ai}'(\beta)|^2 - \beta\text{Ai}^2(\beta)] + \text{Ai}(\beta)\text{Ai}'(\beta)\} . \tag{4.21}$$

*c. Zero-field excitons* ($f=0$, $J=1$):

$$\epsilon_2 = \frac{C_{13}}{3\pi}\sum_{n=2}^{\infty}\frac{(n-1)(n+1)}{n^5}\delta(E+n^{-2}) + \frac{C_{13}\Theta(E)}{6\pi}\frac{E+1}{1-e^{-2\pi/\sqrt{E}}} . \tag{4.22}$$

### D. Weak-field (Stark-effect) limit ($J=1$, $f\ll 1$)

In the weak-field limit, the usual perturbative Stark-effect theory is applicable, giving quadratic

Stark shifts of the $1s$ exciton and linear shifts and splittings for $n \geq 2$ levels. In three dimensions, we have $E_{1s} = -1 - \frac{9}{8}f^2$ and $E_2 = -\frac{1}{4} \pm 3f$. In two dimensions, the corresponding results are

$$E_{1s} = -4 - \tfrac{21}{512}f^2 , \tag{4.23}$$

$$E_2 = -\tfrac{4}{9} \pm (6/\sqrt{5})(\tfrac{15}{16})^3 f . \tag{4.24}$$

The two-dimensional $1s$ Stark-perturbed wave function is

$$U_{1s} = [4/2\pi(1 + \tfrac{159}{16\,384}f^2)]^{1/2}[1 + \tfrac{1}{8}fx(\tfrac{3}{4} + \rho) + O(f^2)]\, e^{-2\rho} . \tag{4.25}$$

The dipole matrix element connecting two-dimensional $s$ and $p$ states is

$$\begin{aligned}\langle np_x | x | ns\rangle &= -eF\left(\frac{2(n+1)(n+2)}{(n+\frac{1}{2})^3(n+\frac{3}{2})^5}\right)^{1/2}\frac{(n+\frac{3}{2})^2}{4}\int \rho\, d\rho \exp\left[-\rho\left(\frac{1}{n+\frac{1}{2}}+\frac{1}{n+\frac{3}{2}}\right)\right]L_n\left(\frac{2\rho}{n+\frac{1}{2}}\right)[L_n(x) - 2L_{n+1}(x) + L_{n+2}(x)] \\ &= \frac{eF}{4(n+2)}\left(\frac{2(n+1)(n+2)}{(n+\frac{1}{2})^3(n+\frac{3}{2})}\right)^{1/2}\frac{d}{d\sigma}\left(\frac{\Gamma(2n+1)}{(n!)^2}\,\frac{(-1)^n\tau^{2n}}{\sigma^{2n+1}}F[-n, -n; -2n; (\sigma/\tau)^2]\right. \\ &\quad - 2\,\frac{\Gamma(2n+2)}{n!\,(n+1)!}\,\frac{(-1)^n\tau^{2n+1}}{\sigma^{2n+2}}F[-n-1, -n; -2n-1; (\sigma/\tau)^2] \\ &\quad \left. + \frac{\Gamma(2n+3)}{n!\,(n+2)!}\,\frac{(-1)^n\tau^{2n+2}}{\sigma^{2n+2}}F[-n-2, -n; -2n-2; (\sigma/\tau)^2]\right) ,\end{aligned} \tag{4.26}$$

where we have;

$$x = \frac{2\rho}{n+\frac{3}{2}}, \quad \sigma = \frac{1}{n+\frac{1}{2}} + \frac{1}{n+\frac{3}{2}}, \quad \tau = \frac{1}{n+\frac{1}{2}} - \frac{1}{n+\frac{3}{2}}, \quad \text{and } \Gamma(n) = (n-1)!$$

$F[n_1, n_2; n_3; u]$ is the Gauss hypergeometric series, normalized as in Ref. 18.

The $1s$ Stark-effect energies are plotted in Fig. 1 as dashed lines both for two and three dimensions. The perturbation theory of that level is valid for $f < 2.5$ in two dimensions and for $f < 0.4$ in three dimensions. The two-dimensional exciton is more tightly bound, less polarizable, and therefore less easily ionized by the same field. Note that in both two and three dimensions the $1s$ exciton shifts to lower energy in a weak field, but as it broadens with increasing field, its peak shifts to *higher* energy, eventually moving into the continuum.

### E. Ultrastrong field limit ($f \gg 1$)

At extremely strong fields $f \gg 1$, the Coulomb interaction is dominated by the applied field, and what had been the $1s$ peak appears as the first peak of the Franz-Keldysh oscillations at energies.

$$E = 3.711 f^{2/3} \quad \text{in two dimensions}, \tag{4.27}$$

and

$$E = 2.338 f^{2/3} \quad \text{in three dimensions}. \tag{4.28}$$

These asymptotic curves are depicted as dotted lines in Fig. 1. Note that even for large fields $f \approx 100$ the numerical calculations (solid lines) do not yet reproduce the ultra-strong field limit, which can only be reached for $f^{1/3} \gg 1$, that is for fields so large that they are experimentally inaccessible: $f \gg 100$.

## V. COMPARSION BETWEEN TWO- AND THREE-DIMENSIONAL ELECTROABSORPTION LINE SHAPES

### A. Allowed direct transitions

The (unbroadened) allowed excitonic ($J = 1$) absorption for two and three dimensions is depicted in Figs. 2(a) and 2(b) for reduced fields $f = 0$, 1, and 3. The zero-field one-electron ($J = 0$) results

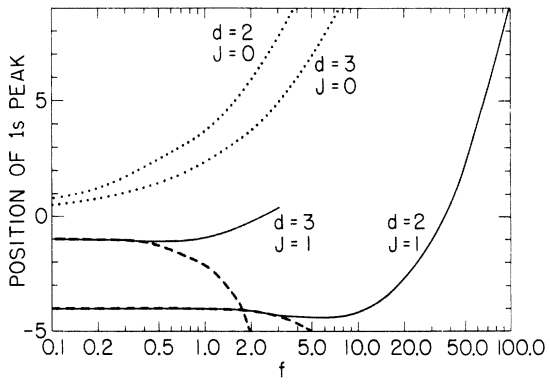


FIG. 1. Computed positions of the $1s$ exciton absorption peak (solid curves) vs $\log_{10} f$ for $d = 2, 3$. The small-field limit [Eq. (4.23)] are shown by the dashed curves, and the Franz-Keldysh limit [calculated from the derivatives of Eqs. (4.6) and (4.10)] is shown by the dotted lines.

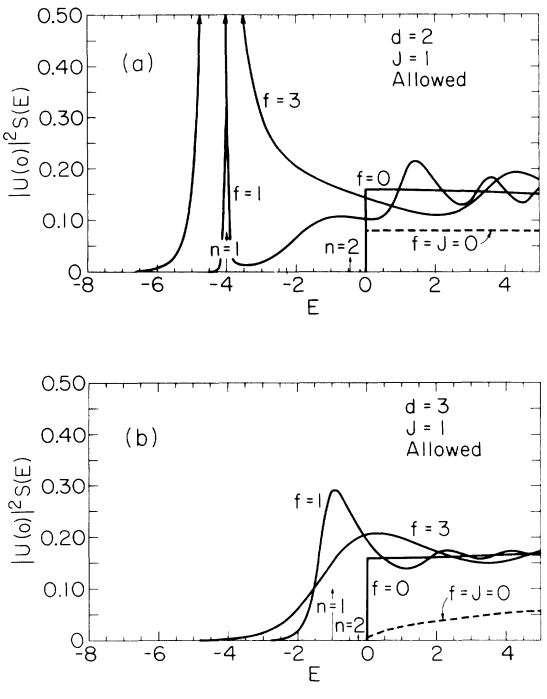


FIG. 2. Allowed absorption $|U(0)|^2S(E)$ for (a) $d=2$ and (b) $d=3$ plotted vs $E \equiv (\hbar\omega - E_{gap})/R$ for $f=0$, 1, 3. The zero-field one-electron limit is shown by the dashed lines. The unbroadened zero-field excitons are $\delta$ functions indicated by arrows.

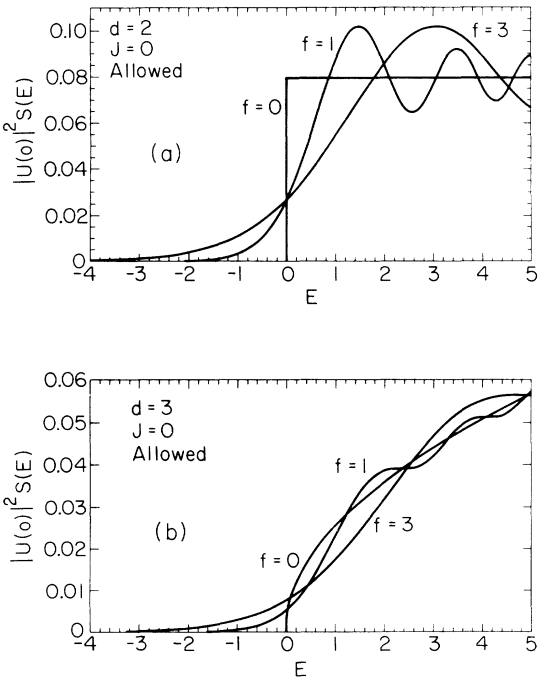


FIG. 3. Franz-Keldysh effect (zero electron-hole interaction: $J=0$) for allowed transitions computed for (a) $d=2$ and (b) $d=3$ with $f=0$, 1, and 3.

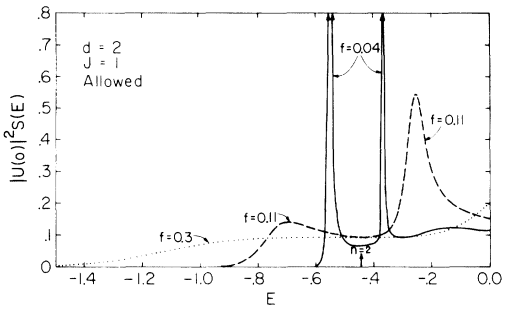


FIG. 4. Computed electroabsorption for $d=2$, $f \ll 1$, near the $n=2$ level. The linear Stark-shift splitting is given in Eq. (4.24) for small fields. For larger fields the $n=2$ state is ionized.

are also depicted in those figures as dashed lines. Corresponding curves for the finite-field one-electron theory are given in Figs. 3(a) and 3(b). Note that in both dimensions the electron-hole Coulomb interaction enhances the absorption over the one-electron result, producing bound states at energies $E_n = -R/[n-\frac{1}{2}(3-d)]^2$ which join on continuously to the Coulomb-enhanced continuum. For a particular field strength, the remnants of the bound excitons are much more pronounced in two dimensions than in three; the classical ionization field for the $n$th exciton $f_c \equiv \epsilon |E_n|^4/4|e|^2 = \{8[n-\frac{1}{2}(3-d)]^4\}^{-1}$ is larger in two dimensions than in three and so the excitons are less easily ionized by an applied field. Even for fields such as $f=3$, well above the classical ionization field, a well-defined excitonic resonance persists below the band gap.

In Fig. 4, we display the two-dimensional weak-field excitonic absorption ($f<1$, $J=1$) in the vicinity of the $2s$ exciton. For $f=0.04$, the $n=2$ Stark doublet is visible with its center shifted slightly to lower energy and a splitting nearly equal to the perturbation theory value. For the larger fields, the $2s$ exciton is thoroughly ionized.

The ionization of the two-dimensional $1s$ exciton is documented in Fig. 5 for large fields $f>1$. Corresponding figures for three dimensions have been published previously by Ralph[9] and by Blossey.[8]

### B. "Forbidden" (second-class) direct transitions

The absorption strength for direct forbidden transitions in two and three dimensions is given in Figs. 6 and 7 including the electron-hole interaction ($J=1$) and neglecting it ($J=0$) for reduced fields. $f=0$, 1, and 3 and for light polarized along the direction of the field. Note the weak field-induced peaks associated with the $n=1$ exciton [in Figs. 6(a) and 6(b)]. The applied field mixes some "$p$" wave function into the $1s$ state giving it a finite oscillator strength for "forbidden" transitions. Note also that the forbidden $1s$ exciton peaks occur at

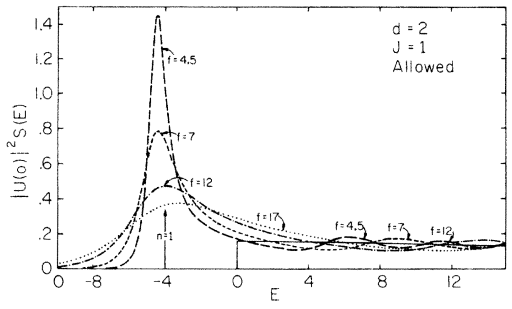


FIG. 5. Allowed excitonic two-dimensional spectrum for larger fields. As the field increases, the $1s$ peak becomes more ionized (broadened) and shifts to higher energies.

different energies than the corresponding allowed peaks [Figs. 2(a) and 2(b)].

For light polarized perpendicular to the applied field the field-induced change in the absorption spectrum is small; therefore we have plotted the (unbroadened) difference between finite-field and zero-field absorption for this case (Figs. 8 and 9).

The results for three-dimensional forbidden

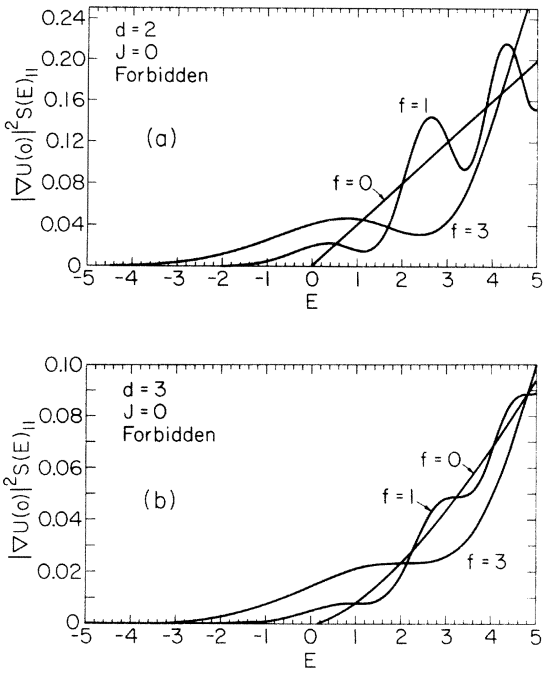


FIG. 7. Franz-Keldysh effect ($J=0$) for forbidden transitions with $\hat{\epsilon} \parallel \vec{F}$ for (a) $d=2$ and (b) $d=3$ with $f=0$, 1, and 3.

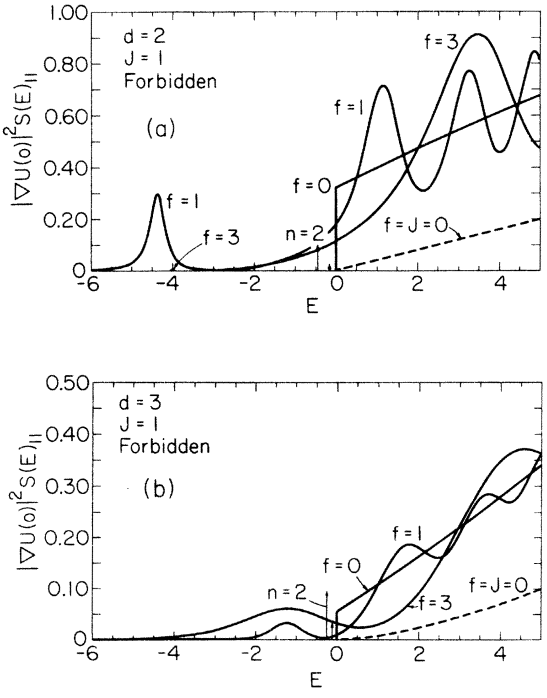


FIG. 6. Computed absorption $|\nabla U(0)|^2 S(E)$ for "forbidden" transitions with photon polarization $\hat{\epsilon}$ parallel to the electric field $\vec{F}$. (a) for $d=2$ and (b) for $d=3$ and reduced fields $f=0$, 1, and 3. The bound exciton positions are denoted by arrows. Note the remnant of the $n=1$ exciton, which becomes allowed in the applied field.

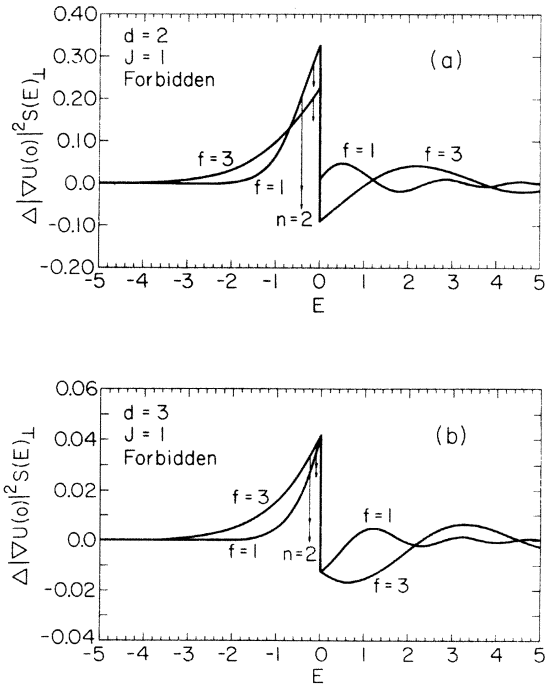


FIG. 8. Plot of $\Delta\epsilon_2/C_0 \equiv [\epsilon_2(\omega, F) - \epsilon_2(\omega, 0)]/C_0$ for forbidden transitions with $\hat{\epsilon} \perp \vec{F}$ (a) for $d=2$ and (b) for $d=3$ with $f=0$, 1, and 3. The arrows show the relative oscillator strengths of absorption by the $\delta$ function bound states.

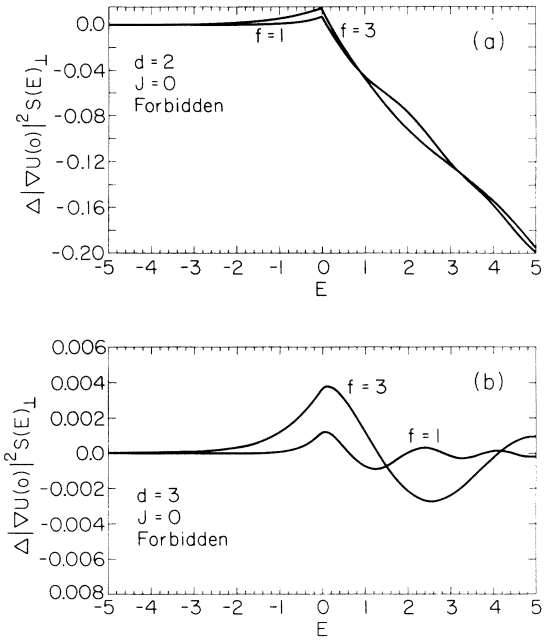


FIG. 9. Plot of $\Delta\epsilon_2$ for $J=0$ (Franz-Keldysh) for forbidden transitions with $\hat{\epsilon} \perp \vec{F}$ for (a) $d=2$ and (b) $d=3$, with $f=0$, 1, and 3.

transitions constitute a set of predictions for the strong-field electroabsorption spectrum of $Cu_2O$.

### C. Indirect transitions

The principle of momentum conservation demands that an annihilated photon transfer all its momentum to the excitation it creates leaving an excitation with virturally zero wave vector $K=2\pi/\lambda \approx 0$. For direct transitions, the light excites only electronic states. For indirect transitions, both the lattice and the electrons are excited, the combined excited state having zero momentum ($\hbar K \approx 0$). However, in general, a range of nonzero center-of-mass electronic momenta $-\hbar\vec{Q}$ is possible with the lattice recoiling to produce net zero momentum for the total excitation. The opening of this center-of-mass channel brings in the center-of-mass density of states. Thus the indirect absorption is to be obtained by convolving the Elliott theory of direct transitions with the density of center-of-mass states[22]:

$$\epsilon_2(\mathcal{E}) = \int_{-\infty}^{\mathcal{E}} \epsilon_2(x)\, dx \ . \tag{5.1}$$

Here we have $\mathcal{E} = \hbar\omega - E_{gap} \mp \hbar\Omega_{\vec{Q}}$, where $\hbar\Omega_{\vec{Q}}$ is the energy of the phonon responsible for the indirect transition. For two-dimensional excitons in zero field this yields a series of step functions for $\mathcal{E}<0$ (see Fig. 10):

$$\epsilon_2 = \frac{C_{02}}{\pi} \sum_{n=1}^{\infty} \frac{1}{(n-\frac{1}{2})^3}\, \Theta\left(\mathcal{E} + \frac{1}{(n-\frac{1}{2})^2}\right). \tag{5.2}$$

The finite-field electroabsorption has been computed for $f=3$ and so nearly equals the zero-field absorption that we show the differential absorption $\Delta\epsilon_2 = \epsilon_2(\mathcal{E}, f) - \epsilon_2(\mathcal{E}, 0)$ in Fig. 11. It is noteworthy that Kamimura *et al.* have interpreted GaSe data in terms of an indirect transition model; hence, under appropriate (difficult) experimental conditions, electroabsorption data and the theory of Fig. 11 could be used to test this interpretation and to determine band parameters of such materials in the manner of earlier three-dimensional exciton work.[23,24]

## VI. INTERPOLATION OF THEORETICAL CURVES

In most experiments, one measures the direct allowed differential absorption $\Delta\epsilon_2(\omega, F) \equiv \epsilon_2(\omega, F) - \epsilon_2(\omega, 0)$ and easily determines the positions of spectral nodes and antinodes for $\hbar\omega > E_{gap}$, as functions of applied field strength. To facilitate comparison with such data, we exhibit in Fig. 12 the calculated positions of these nodes and antinodes

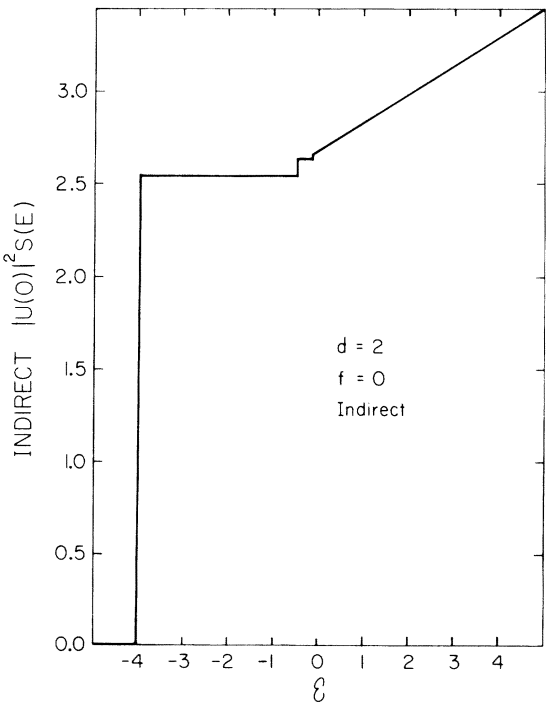


FIG. 10. Zero-field indirect electroabsorption for $d=2$. The series of step functions for $\hbar\omega - E_{gap} - \hbar\Omega_{\vec{Q}} \equiv \mathcal{E} < 0$ result from the convolution of the bound-state $\delta$ functions with the center-of-mass density of states [see Eq. (5.2)].

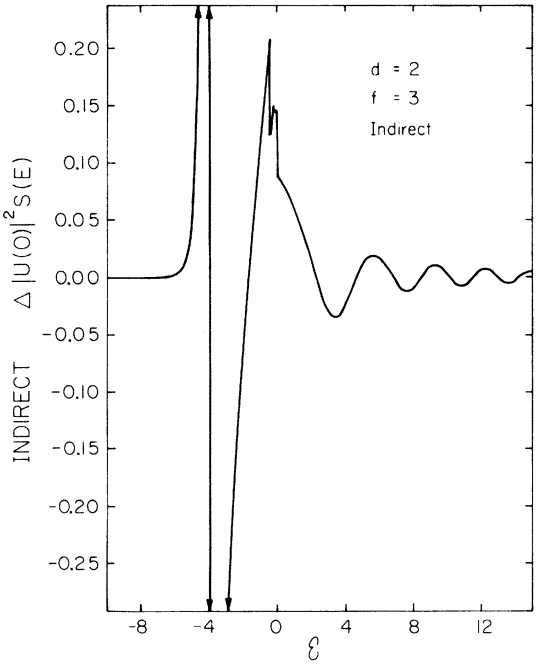


FIG. 11. Computed differential absorption $\Delta\epsilon_2(\mathcal{E},f)/C_{02}$ plotted vs $\mathcal{E}$ for $f=3$, $d=2$ allowed indirect transitions.

as functions of $f$. If we define $E(n,f)$, the position of the $n$th node or antinode, then an adequate approximation to the curves in Fig. 12 is

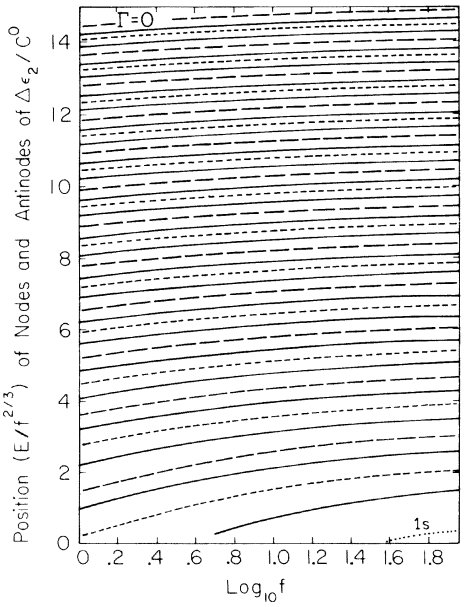


FIG. 12. Computed position $(E/f^{2/3})$ of nodes (solid lines), relative maxima (long dashed lines), and relative minima (short dashed lines) of $\Delta\epsilon_2 \equiv \epsilon_2(\omega,f)-\epsilon_2(\omega,0)$ for $d=2$ allowed absorption plotted vs $\log_{10}f$. The $1s$ exciton peak moves into the continuum for $f \lesssim 35$, (i.e., $\log_{10}f > 1.55$) and is denoted by a dotted line.

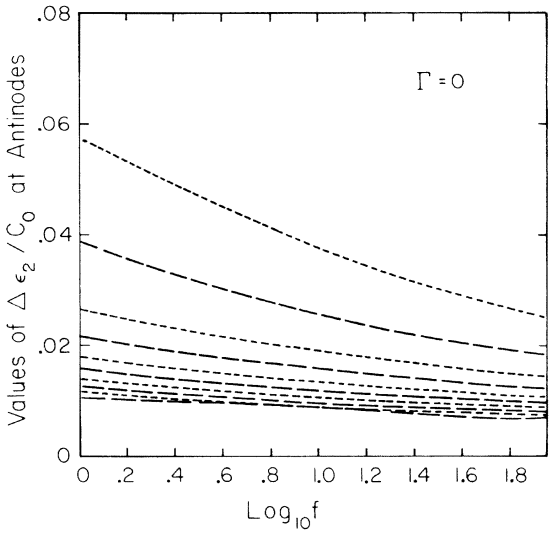


FIG. 13. Computed absolute values of $\epsilon_2/C_0$ at the maxima (long dashed) and minima (short dashed) for $d=2$ plotted vs $\log_{10}f$. The solid lines are calculated from Eq. (6.3) and Table II.

$$E(n,f)=f^{2/3}\sum_{i=1}^{5}\sum_{j=1}^{5}B_{ij}(\log_{10}n)^{i-1}(\log_{10}f)^{j-1}, \tag{6.1}$$

where the coefficients $B_{ij}$ are listed in Table I. In Eq. (6.1), $n=1$, 3, 5 corresponds to the first, second, and third nodes (for $E>0$), $n=2$, 6, 10 correspond the minima in $\Delta\epsilon_2$ and $n=4$, 8, 12 correpond to maxima.

These results are appropriate for weak Lorentzian broadening[25]: $\Gamma \ll R$, $\Gamma \ll fR$; corresponding results for larger values of $\Gamma$ are available elsewhere.[26] For $f \gtrsim 1$ and $\hbar\omega < E_{gap}$, the structure in $\Delta\epsilon_2(\omega,f)$ is normally dominated by the zero-field (broadened) excitons, because $\epsilon_2(\omega,F)$ is a smooth function of $\hbar\omega$, having only a broad peak reminiscent of the bound $1s$ exciton state.

The function

$$\mathcal{L}(\omega)=\Delta\epsilon_2(\omega,F)=A(\omega,F)\cos\theta(\omega,F) \tag{6.2}$$

oscillates as a function of photon energy $\hbar\omega$; the absolute value of the envelope function $A(\omega,F)$ oscillations is given in Fig. 13. An approximation to the curves in Fig. 13 is

TABLE I. Fitting coefficients for Eq. (6.1) for approximating the positions of nodes and antinodes of allowed electroabsorption. See Fig. 12.

| $B_{ij}$ | $j=1$ | $j=2$ | $j=3$ | $j=4$ | $j=5$ |
|---|---|---|---|---|---|
| $i=1$ | −1.9399 | 4.8579 | −3.0939 | 1.0890 | −0.1599 |
| $i=2$ | 7.5343 | −12.2872 | 9.4288 | −3.3546 | 0.4477 |
| $i=3$ | −4.7430 | 16.2927 | −12.7541 | 4.2151 | −0.4735 |
| $i=4$ | 3.5909 | −10.3473 | 7.9910 | −2.5118 | 0.2497 |
| $i=5$ | 0.0090 | 2.4142 | −1.8339 | 0.5574 | −0.0508 |

TABLE II. Fitting coefficients for Eq. (6.3) for allowed electroabsorption amplitude $A[E(n,f),f]$. See Fig. 13.

| $A_{ij}$ | $j=1$ | $j=2$ | $j=3$ | $j=4$ | $j=5$ |
|---|---|---|---|---|---|
| $i=1$ | 0.5753 | −0.0213 | −0.0001 | 0.0019 | −0.0003 |
| $i=2$ | −0.0420 | 0.0217 | −0.0841 | 0.0886 | −0.0248 |
| $i=3$ | −0.1256 | −0.0438 | 0.5945 | −0.5872 | 0.1587 |
| $i=4$ | 0.2177 | 0.1234 | −1.0770 | 1.0341 | −0.2774 |
| $i=5$ | −0.0969 | −0.0837 | 0.5724 | −0.5430 | 0.1454 |

$$A(E(n,f),f)=\sum_{i=1}^{5}\sum_{j=1}^{5}A_{ij}(\log_{10}\tfrac{1}{2}n)^{i-1}(\log_{10}f)^{j-1}\,, \tag{6.3}$$

where the coefficients $A_{ij}$ are listed in Table II and are the same as in Eq. (6.1).

## VII. SUMMARY

A principal obstacle to a complete theory of electroabsorption in anisotropic semiconductors has been removed; it is now possible to compute electroabsorption line shapes for two-dimensional excitons. These solutions can be combined with the adiabatic approximation[27] to generate approximate line shapes for electroabsorption by anisotropic three-dimensional semiconductors (large, but finite mass $M_z$).

## APPENDIX

In two dimensions, the following equations replace the corresponding equations of Sec. IV and the Appendix of Ref. 11. (The equation numbers of this latter reference appear in the margin preceded by DR.)

$$(-\nabla_{x,y}^2-2/\rho+fx)U_\nu(x,y)=E_\nu U_\nu(x,y)\,, \tag{DR4.1}$$

$$\xi=\rho+x,\quad \zeta=\rho-x,\quad x=\tfrac{1}{2}(\xi-\zeta),\quad y=\sqrt{\xi\zeta}\,,\quad \rho=\tfrac{1}{2}(\xi+\zeta), \tag{DR4.2}$$

$$U(\vec{\rho})=\chi_1(\xi)\chi_2(\zeta)/(\xi\zeta)^{1/4}\,, \tag{DR4.4}$$

$$K_A=(2\pi e^2/m^2c\eta'\omega)^2\left|\langle c\vec{k}_{0,\parallel}\vec{R}^0_{h\perp}|\,\hat{\epsilon}\cdot\vec{p}\,|v\vec{k}_{0,\parallel}\vec{R}^0_{h\perp}\rangle\right|^2$$

$$\times|U(0)|^2S(E)\,, \tag{DR4.7}$$

$$|U(0)|^2S(E)=\frac{1}{Ra^2}\sum_n\left(A^2\pi^2f^{1/2}\int_0^\infty\chi^2_{1\text{-}UN}(\xi)\xi^{-1}\,d\xi\right), \tag{DR4.8}$$

$$\chi_{1\text{-}UN}=\xi^{(m+1)/2}[1-t\xi/(m+1)+O(\xi^2)]\,, \tag{DRA1}$$

$$d^2\gamma=\tfrac{1}{4}(\zeta/\xi+\xi/\zeta)\,d\xi\,d\zeta\,, \tag{DRA4}$$

$$\frac{1}{4}\int_0^\infty\frac{\chi_1^2(\xi)}{\xi}\,d\xi\int^{L_2}\chi_2^2(\zeta)\,d\zeta=1=\frac{1}{4}\int_0^\infty\frac{\chi_1^2(\xi)}{\xi}\,d\xi\,(2L_2)^{1/2}A^2\,, \tag{DRA7}$$

$$\chi_{2\text{-}UN}(\xi)=\xi^{(m+1)/2}[1+(1-t)\xi/(m+1)+O(\xi^2)]\,, \tag{DRA8}$$

$$\sum_\nu|U_\nu(0)|^2\delta(E-E_\nu)=2\sum_{t,E'}\lim_{\substack{\xi\to0\\\zeta\to0}}\frac{|\chi_1(\xi;t_n,E')\chi_2(\zeta;t_n,E')|^2}{\sqrt{\xi\zeta}}\,, \tag{DRA9}$$

$$K_A=\frac{4\pi e^2}{m^2c\eta'(\omega)\omega}\,\frac{2}{\pi}\left(\frac{L_2}{2f}\right)^{1/2}\times\sum\lim_{\substack{\xi\to0\\\zeta\to0}}\frac{|\chi_1(\xi;t_n,E')\chi_2(\zeta;t_n,E')|^2}{\sqrt{\xi\zeta}}\,, \tag{DRA11}$$

$$K_A=\frac{4\pi e^2}{m^2c\eta'(\omega)\omega}\,2|U(0)|^2S(E)\,, \tag{DRA12}$$

$$|U(0)|^2S(E)=\frac{1}{Ra^2}\sum_{n=0}^{\infty}\left(\pi^2f^{1/2}\times\int_0^\infty\frac{\chi^2_{1\text{-}UN}(\xi;t_n,E)\,d\xi\,A^2(t_n,E)}{\xi}\right)^{-1}. \tag{DRA13}$$

We hereby correct the following typographical errors in Ref. 11: Eq. (2.5) should read $(d/dt)\hbar\vec{k}(t)=e\vec{F}$; the line below Eq. (2.7) should have $\lambda^3=2m^*|e|F/\hbar^2$; and Eq. (A10) should read $\rho(E')=dn/dE'=\pi^{-1}\sqrt{L_2/2f}$.

*Research supported by NSF under Grant Nos. DMR-7203026, GH-33750, and GH-39132.

†Present address: General Electric Corporate Research and Development Center, Schenectady, N. Y. 12301.

[1]F. R. Gamble, J. H. Osiecki, M. Cais, R. Pisharody, F. J. DiSalvo, and T. H. Geballe, Science 174, 493 (1971).
[2]A. W. Overhauser, Phys. Rev. 167, 691 (1968).
[3]S.-K. Chan and V. Heine, J. Phys. F 3, 795 (1973).
[4]J. A. Wilson, F. J. DiSalvo, and S. Mahajan, Phys. Rev. Lett. 32, 882 (1974).
[5]H. Kamimura, K. Nakao, and Y. Nishina, Phys. Rev. Lett. 22, 1379 (1969).
[6]J. Bordas and E. A. Davis, Solid State Commun. 12, 717 (1973).
[7]G. Harbeke and E. Tosatti, Phys. Rev. Lett. 28, 1567 (1972).
[8]D. F. Blossey, Phys. Rev. B 3, 1382 (1971).
[9]H. I. Ralph, J. Phys. C 1, 378 (1968).
[10]B. Y. Lao, J. D. Dow, and F. C. Weinstein, Phys. Rev. B 4, 4424 (1971).
[11]J. D. Dow and D. Redfield, Phys. Rev. B 1, 3358 (1970).
[12]W. Andreoni and R. Del Sole, report (unpublished).
[13]G. Wexler and B. Ricco, report (unpublished).
[14]R. J. Elliott, Phys. Rev. 108, 1384 (1957).
[15]G. A. Korn and T. M. Korn, *Mathematical Handbook for Scientists and Engineers* (McGraw-Hill, New York, 1968), p. 178.
[16]The limit of vanishing electron-hole interaction is achieved by setting $J=0$.

[17]D. E. Aspnes, Phys. Rev. 147, 554 (1966).
[18]M. Abramowitz and I. A. Stegun, *Handbook of Mathematical Functions* (Dover, New York, 1968), p. 775.
[19]M. Shinada and S. Sugano, J. Phys. Soc. Jpn. 21, 1936 (1966).
[20]S. Flügge and H. Marschall, *Reichenmethoden der Quantentheorie* (Springer-Verlag, Berlin, 1965), p. 80.
[21]K. Tharmalingam, Phys. Rev. 130, 2204 (1963).
[22]We note an interesting feature of two-dimensional exciton theory: namely, if conduction and valence bands are parallel but not flat, the reduced mass is infinite, but the total mass is zero. Hence, it is possible to have two-dimensional indirect transitions where the convoluting function is three dimensional rather than two dimensional.
[23]P. Handler, S. Jasperson, and S. Koeppen, Phys. Rev. Lett. 23, 1387 (1969).
[24]S. F. Pond, Ph.D. thesis (University of Illinois, 1971) (unpublished).
[25]$\Delta\epsilon_2(E,\Gamma)=\int_{-\infty}^{\infty} B(E-E',\Gamma)\Delta\epsilon_2(E')\,dE'$, where $B(A,\Gamma)=(\Gamma/\pi)(\Gamma^2+A^2)^{-1}$.
[26]F. L. Lederman, Ph.D. thesis, Ch. 3 (University of Illinois, 1975) (unpublished).
[27]E. O. Kane, Phys. Rev. 180, 852 (1969).